Research Article

Title – Dispensable regulation of brain development and myelination by Serpina3n.

Authors: Meina Zhu, Yan Wang, Joohyun Park, Shuaishuai Gong, Fuzheng Guo

Author affiliation: Department of Neurology, School of Medicine, UC Davis; Institute for Pediatric Regenerative Medicine (IPRM), Shriners Hospitals for Children, Sacramento, CA

Correspondence: Fuzheng Guo, UC Davis School of Medicine/IPRM Shriners hospital Sacramento CA. 2425 Stockton Blvd., Sacramento, CA 95817 Email: fzguo@ucdavis.edu ORCID: 0000-0003-3410-8389

Acknowledgements and declaration: We thank the funding agencies of NIH (R21NS125464, R01NS123080, R01NS123165, R01NS134887) and Shriners Hospitals for Children (85101-NCA-22, 85113-NCA-23). The authors declared no conflict of interest and all consented to publication.

Abstract:

Serine protease inhibitor clade A member 3n (Serpina3n) or its human orthologue SERPINA3 is a secretory glycoprotein expressed primarily in the liver and brain under homeostatic conditions and dysregulated in various CNS pathologies. Yet its cellular expression profile and physiological significance in postnatal development remain elusive. Here, we showed that Serpina3n protein is expressed predominantly in oligodendroglial lineage cells in the postnatal CNS and that oligodendrocytes (OLs) responded to oxidative injury by upregulating Serpina3n production and secretion. Using loss-of-function genetic tools, we found that Serpina3n conditional knockout (cKO) from Olig2-expressing cells did not affect motor and cognitive functions in mice. Serpina3n depletion in Olig2-expressing cells did not appear to interfere with oligodendrocyte differentiation and developmental myelination nor affect the population of other glial cells and neurons *in vivo*. *In vitro* primary cell culture showed that Serpina3n-sufficient and -deficient oligodendroglial progenitor cells (OPCs) differentiated into myelin gene-expressing OLs comparatively. Together, these data suggest that Serpina3n plays a minor role, if any, in regulating brain neural cell development and myelination under homeostatic conditions and raise interests in pursuing its functional significance in CNS diseases and injuries.

Introduction

Human SERPINA3 (also known as anti-chymotrypsin, ACT), one of the members of the serine protease inhibitor (Serpin) superfamily, is expressed mainly in the liver and brain under homeostasis (www.proteinatlas.org) and its primary molecular function of which is to inhibit the proteolytic activity of endogenous serine protease enzymes (Sanchez-Navarro et al., 2021). SERPINA3 is an acute phase glycoprotein that is secreted primarily by the liver to the bloodstream in response to injury/infection (Jain et al., 2011) and is elevated in the plasma and/or cerebrospinal fluid of patients affected by cancers (de Mezer et al., 2023) and neurological diseases/injuries such as Alzheimer's disease (DeKosky et al., 2003) and multiple sclerosis (Fissolo et al., 2021). SERPINA3 also displays DNA binding properties and has been reported to function as a transcription regulator (Ko et al., 2019; Ko et al., 2018) and epigenetic modulator (Santamaria et al., 2013). The role of SERPINA3 in regulating neurological disease pathophysiology remains underdefined partially due to lack of genetic animal tools.

Murine Serpina3n was identified as the orthologue of human SERPINA3 based on structural and functional similarities (Horvath et al., 2005), open the possibility to use genetic modified Serpina3n to study its role in brain development and CNS diseases. In the CNS, Serpina3n mRNA has been widely cited as a marker for reactive astrocytes in response to neuroinflammation and ischemic stroke (Zamanian et al., 2012). However, recent unbiased transcriptomic data suggest that Serpina3n is upregulated primarily in oligodendroglial lineage cells under various disease/injury conditions (Kenigsbuch et al., 2022), suggesting that it may regulate oligodendrocyte biology and pathology. Recently, SERPINA3/Serpina3n has been shown to be expressed in embryonic radial glia cells and play a crucial role in brain development and cognitive function in mice (Zhao et al., 2022). It remains elusive if Serpina3n is expressed in the CNS during postnatal development under homeostatic conditions and its functional significance in postnatal brain development and animal behavior.

In this study, we sought to tackle these questions by employing Cre-loxP-mediated genetic approaches. We first reported that oligodendroglial lineage cells are the primary cell type in the CNS white matter expressing Serpina3n protein under physiological circumstances and respond to oxidative stress by upregulating and secreting Serpina3n. Using Olig2-Cre line to deplete Serpina3n in Olig2-expressing neural precursors and their neural progenies (mainly oligodendroglial lineage cells), we found that physiological Serpina3n appears to be dispensable for oligodendroglial development and myelination. Serpina3n-deficienct mice develop normal motor and cognitive functions and display undistinguishable development in other glial cells and

neurons. Given that Serpina3n is the top signature gene marking disease-associated oligodendrocytes detected in various CNS pathologies (Kenigsbuch *et al.*, 2022), our study provided a valuable genetic tool to study the nature and function of Serpina3n-expressing oligodendroglia under diseased/injured conditions.

Results

1. Serpina3n expression in oligodendroglial lineage cells both in vitro and in vivo

Given its expression in the brain and its upregulation predominantly in oligodendroglia among various CNS pathologies (Kenigsbuch *et al.*, 2022), we asked if Serpina3n is expressed in homeostatic oligodendroglial lineage cells. Using primary culture of oligodendrocyte progenitor cells (OPCs) purified from neonatal murine brain, we showed Serpina3n expression in OPCs and upregulation in differentiating OLs at the mRNA level (**Fig. 1A**). Western blot assays demonstrated the high-level expression of the protein product along oligodendroglial lineage progression (**Fig. 1B**). Of Note, the differential temporal regulation of Serpina3n mRNA (**Fig. 1A**) and protein (**Fig. 1B**) suggests that Serpina3n mRNA level may not be a bode fide indicator of the protein production. Serpina3n is a glycoprotein harboring an N-terminal secretion peptide signal (Vicuna et al., 2015). To test its upregulation and secretion from OLs, primary OLs were incubated with hydrogen peroxide (H_2O_2), an established inducer of oxidative injury for 24 hours (**Fig. 1C**). Oxidative injury was verified by the significant reduction in the expression of oligodendroglial marker Sox10 (**Fig. 1D**) and by the marked upregulation of the oxidative stress transcription factor NRF2 (gene symbol *Nfe2l2*) (Ma, 2013) (**Fig. 1E, left**) and NRF2's target gene Hmox1 (**Fig. 1E, right**). Our data showed that OLs responded to oxidative stress by significantly upregulating Serpina3n expression (**Fig. 1F**). Importantly, Serpina3n secretion was detected under the non-injury control condition yet significantly increased under injury condition (**Fig. 1G**). These data suggest that OL may express and secrete Serpina3n. Concomitant with Serpina3n upregulation, cell senescence markers P16 and P21 (**Fig. 1H**) (Wagner and Wagner, 2022) and the complement C1q (**Fig. 1I**), which plays a crucial role in normal brain development (Rupprecht et al., 2021), were significantly induced from injured OLs. Taken together, these data suggest that homeostatic OLs express and secrete Serpina3n, both of which are dysregulated under injured conditions.

Figure 1 - Serpina3n is expressed in primary oligodendroglia and responds to injury in vitro.

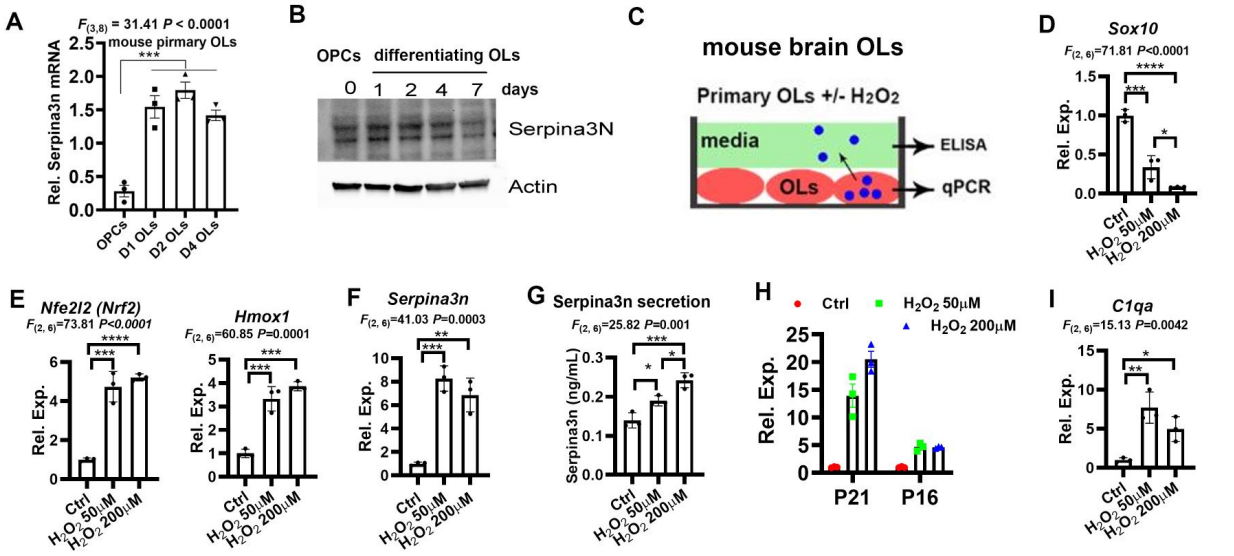

A, RT-qPCR assay for Serpina3n mRNA in primary mouse OPCs and differentiating OLs at day 1 (D1), D2, and D4 in differentiation media. **B**, Western blot assay for Serpina3n protein in primary rat OLs at different time points. **C**, experimental design for panels **D-I**. Primary mouse OLs at D0 were injured by 50μM or 200 μM hydrogen peroxide H_2O_2 for 24 hours **D**, RT-qPCR assay for oligodendroglial marker Sox10 mRNA. **E**, RT-qPCR assay for the oxidative stress transcription factor NRF2 and its target gene Hmox1. **F**, RT-qPCR assay for Serpina3n mRNA. **G**, ELISA assay for Serpina3n secretion in culture media. H-I, RT-qPCR assay for the expression of the cell senescence markers p21 and p16 (**H**) complement C1q (**I**) in H_2O_2-treated OLs. One-way ANOVA followed by Tukey's multiple comparison test, * P<0.05, ** P<0.01, *** P<0.001, **** P<0.0001.

To confirm Serpina3n expression in oligodendroglial lineage cells in vivo, we used cold-methanol-fixed cryosections prepared from the early postnatal CNS. Double fluorescence immunohistochemistry (IHC) demonstrated that Serpina3n protein was clearly expressed in cells labeled by the monoclonal antibody CC1, an established OL marker, in the CNS for example the spinal cord (**Fig. 2A1**) and the brain corpus callosum (**Fig. 2B1**), albeit at the low level. In the spinal white matter tract, approximately 50% of $CC1^+$ cells displayed Serpina3n immunoreactive signals and virtually all $Serpina3n^+$ cells were CC1 positive. To verify the authentication of Serpina3n immunoreactive signals, Serpina3n conditional knockout (cKO) mice were generated by crossing Serpina3n-floxed mice with widely-used oligodendroglial cell targeting Olig2-Cre line. *Olig2-Cre:Serpina3n*$^{fl/fl}$ was referred to as Serpina3n cKO mice whereas *Olig2-Cre:Serpina3n*$^{fl/+}$, Olig2-Cre, and/or Serpina3n$^{fl/fl}$ as Ctrl mice. Our data showed that the low level Serpina3n immunoreactive signals were mostly abolished in $CC1^+$ OLs of Ctrl mice (**Fig. 2 A2, B2**). Purified OLs were isolated by magnetic-assisted cell sorting (MACS)

(Zhang et al., 2021a) (cf Fig. 10) from Serpina3n Ctrl and cKO brain. To further prove the cellular specificity of Sepina3n cKO, we observed a significant reduction of Serpina3n mRNA in isolated OLs (**Fig. 2C**) but not in astrocytes (**Fig. 2D**). These data altogether demonstrate that Serpina3n is expressed primarily in oligodendrocytes in the early postnatal brain and that our Serpina3n is effectively ablated in oligodendrocytes of Serpina3n cKO mice.

Figure 2 - Serpina3n expression and conditional knockout in the CNS.

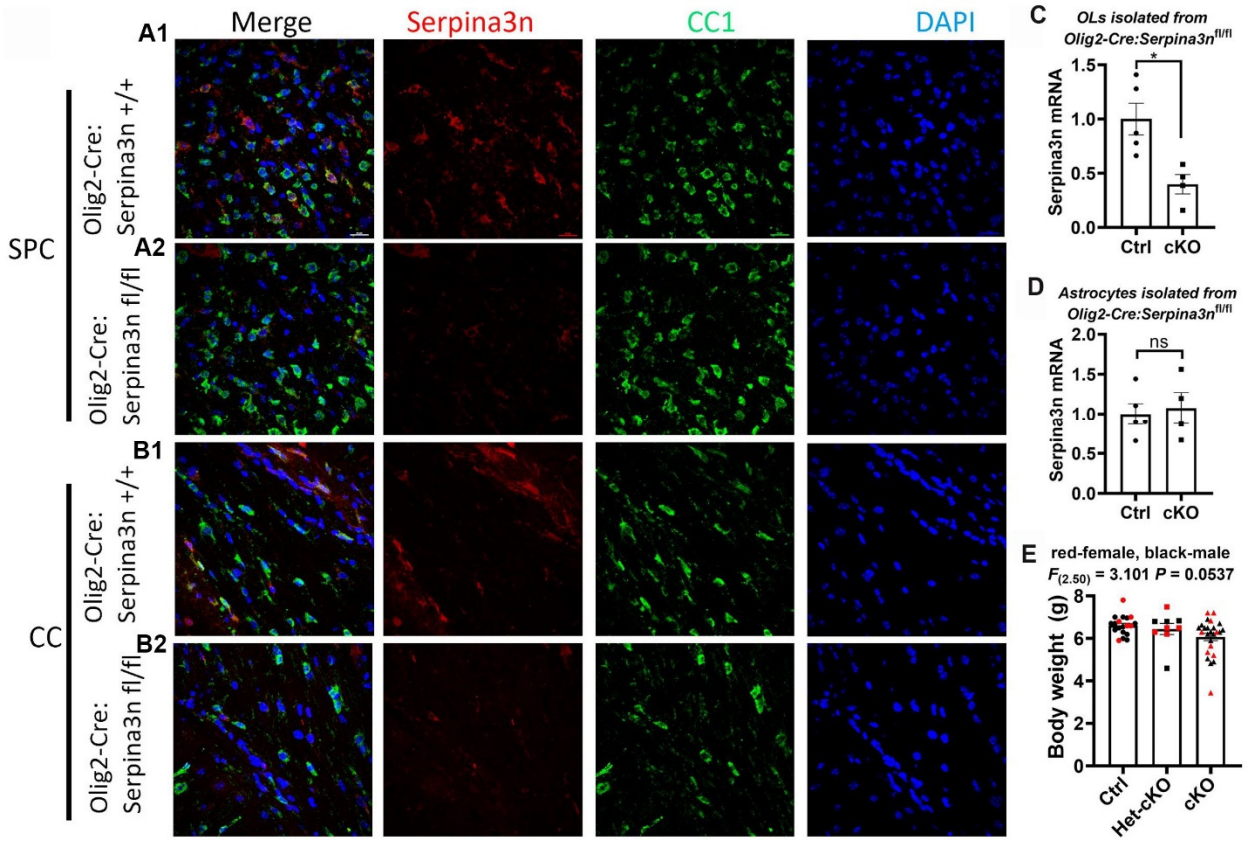

A1-B2, Serpina3n protein expression in CC1-positive OLs in the spinal cord (SPC, A1, A2) and corpus callosum (CC) (B1, B2) evidenced by fluorescent immunohistochemistry (IHC). Note that Serpina3n immunoreactive signal was eliminated in Serpina3n cKO mice. **C**, RT-qPCR assay for Serpina3n in OLs acutely isolated by magnetic-assisted cell sorting (MACS, O4-magnetic beads) from P10 brain of Serpina3n cKO and Ctrl mice. Two-tailed Student's t test, t=3.285, df=7, * $P<0.05$. **D**, RT-qPCR assay for Serpina3n in astrocytes acutely isolated by MSCS (ACSA2-magnetic beads) from P10 brain of Serpina3n cKO and Ctrl mice. Two-tailed Student's t test, t=0.3281, df=7, $P=0.7525$. **E**, body weight of P14 mice. one-way ANOVA. *Olig2-Cre:Serpina3n*$^{fl/fl}$ (Serpina3n cKO), *Olig2-Cre:Serpina3n*$^{fl/+}$ (Serpina3n het-cKO) or *Olig2-Cre:Serpina3n*$^{+/+}$ (Serpina3n Ctrl) mice were analyzed at postnatal day 10 (P10) in **panel A1-D** and P14 in **panel E.** Scale bars = 10 µm.

2. Serpina3n-deficient mice develop comparable motor and cognitive function to control mice

Serpina3n cKO mice were born in expected Mendelian ratios and fertile. No gross growth abnormalities were observed throughout their postnatal development. The body weight of Serpina3n cKO mice were slightly reduced compared to Ctrl mice at P14, but the difference was not statistically significant (**Fig. 2E**). Accelerating Rotarod test was used to evaluate their motor function and no difference in the motor performance was observed during the training (**Fig. 3A**) and probe (**Fig. 3B**) sessions between Serpina3n cKO and Ctrl mice. Serpina3n cKO mice also displayed normal ability of motor learning compared to controls (**Fig. 3C**). Sensitive CatWalk test with automatic video-tracking was used to test the walking gait (Wang et al., 2022). The overall walking gait was unaffected by Serpina3n deficiency evidenced by comparable gait regularity index (**Fig. 3D**). The base of support of two front paws appeared to be affected by Serpina3n deficiency (**Fig. 3E**). However, the impairment was not seen in the hind paw of Serpina3n cKO mice (**Fig. 3F**). These data suggest that oligodendroglial Serpina3n seems to play a minor role in animal motor behavior.

Figure 3 – motor function of Serpina3n-deficient mice

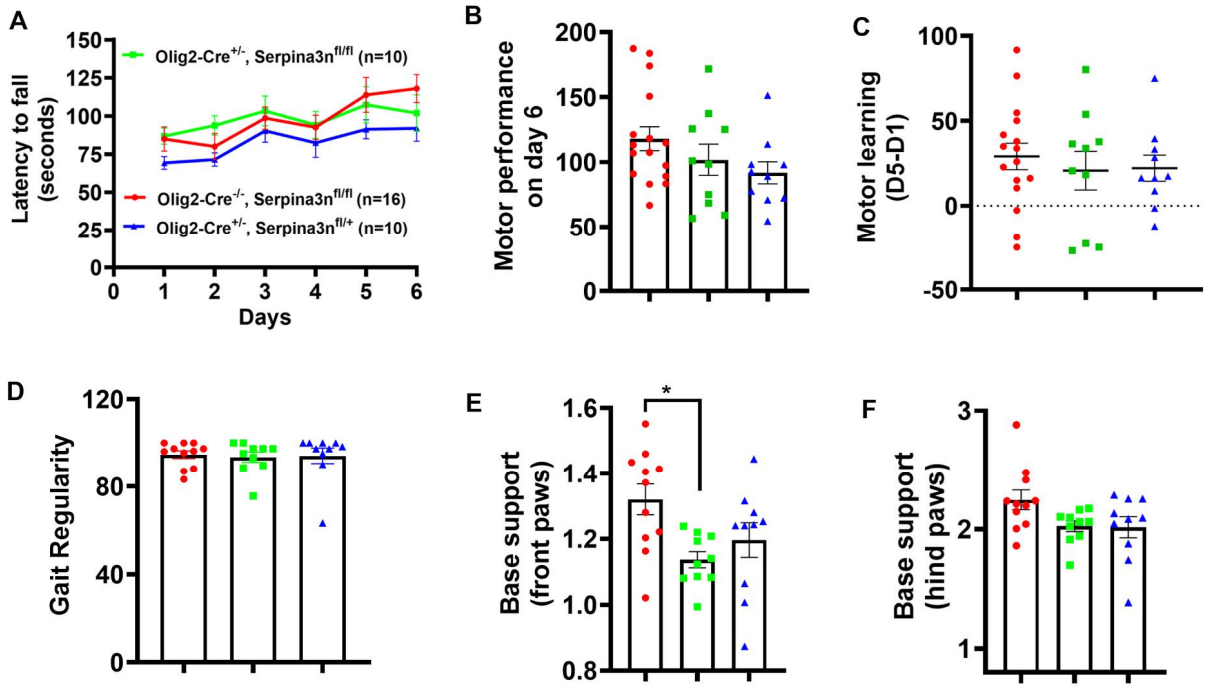

A-C: motor function assessed accelerating Rorarod test; **D-F**: Gait analysis assessed by Noldus Catwalk. **A**, time-course of latency to fall (seconds) of mice during accelerating Rotarod test. Two-way ANOVA, time-course $F_{(3.4, 112.5)}$=10.29, P<0.0001; genotype $F_{(2, 33)}$=1.323, P=0.2801. **B**, motor performance on day 6 (latency to fall). One-way

ANOVA, $F_{(2, 33)}$=1.323, P=0.2801. **C**, motor learning ability (changes in latency to fall). One-way ANOVA, $F_{(2, 33)}$=0.2811, P=0.7567. **D**, gait regularity index. One-way ANOVA, $F_{(2, 28)}$=0.0531, P=0.9484. **E-F**, the base of support (the average width of two paws when walking) for front (**E**) and hind (**F**) paws (unit, centimeter). One-way ANOVA, front paws $F_{(2, 28)}$=4.743, P=0.0168, hind paws $F_{(2, 28)}$=3.115, P=0.0601, * P<0.05, Tukey's multiple comparison test

Figure 4 – Uninterrupted cognitive function of Serpina3n cKO mice.

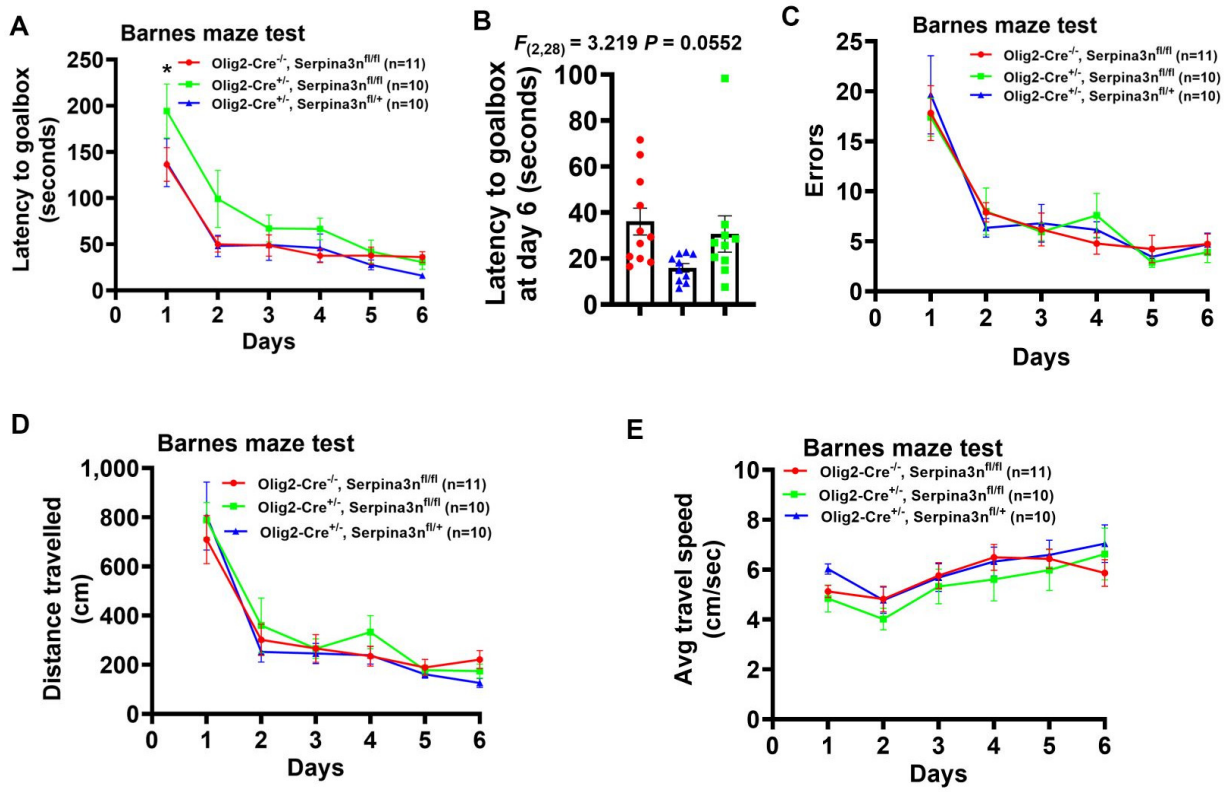

A, time latency (seconds) prior to entering the goalbox. Time course $F_{(5, 168)}$=27.37, P<0.0001, genotype $F_{(2, 168)}$=6.2037, P=0.0025. * P<0.05 at Day 1. **B**, Latency to goalbox tested on day 6. **C**, number of errors made prior to goalbox. Time course $F_{(5, 168)}$=29.38, P<0.0001, genotype $F_{(2, 168)}$=0.037, P=0.9637. **D**, total distance travel during test. Time course $F_{(5, 168)}$=38.50, P<0.0001, genotype $F_{(2, 168)}$=0.7992, P=0.4523. **E**, average moving speed during test. Time course $F_{(5, 168)}$=4.554, P=0.0006, genotype $F_{(2, 168)}$=1.819, P=0.1654. Two-way ANOVA except B, one-way ANOVA.

We next employed Barnes Maze test to assess animal spatial learning function (Wang *et al.*, 2022). The baseline cognition seemed to be initially impaired for Serpina3n cKO mice compared to Ctrl mice (Day 1 and day2), assessed by increased time latency to goalbox (**Fig. 4A**). However, both Serpina3n cKO and Ctrl mice displayed remarkable improvement yet indistinguishable spatial learning ability during the subsequent training and probe sessions (**Fig.**

A-C). Importantly, no difference was observed in total distance traveled (**Fig. 4D**) or average travel speed (**Fig. 4E**) during 5-minute sessions, suggesting that Serpina3n deficiency does not alter motor function. Taken together, these data suggest that Serpina3n plays a minor role in animal motor or cognitive function during postnatal development.

3. Normal oligodendrocyte differentiation in Serpina3n-deficient mice

We next sought to evaluate the potential effects of Serpina3n depletion on oligodendrocyte differentiation. To this end, triple fluorescence IHC of SOX10, PDGFRa, and CC1 (**Fig. 5A**). The densities of total oligodendroglial lineage cells ($SOX10^+$), OPCs ($SOX10^+/PDGFRa^+$), and differentiated OLs ($SOX10^+/CC1^+$) was quantified from different CNS regions. We chose P15 for the quantification since oligodendroglial differentiation peaks in the CNS of this time window. Our thorough quantification failed to reveal a significant difference in the number of oligodendroglial lineage cells (**Fig. 5B**), OPCs (**Fig. 5C**) or differentiated OLs (**Fig. 5D**) in various CNS white matter tracts, except for the subcortical white matter tract where the density of OLs appeared to very slightly yet significantly increased in Serpina3n cKO mice compared to Ctrl mice (**Fig. 5D**). These data indicate that Serpina3n may play a minor role, if any, in oligodendroglial differentiation throughout the CNS.

Figure 5 – oligodendrocyte differentiation during postnatal CNS development.

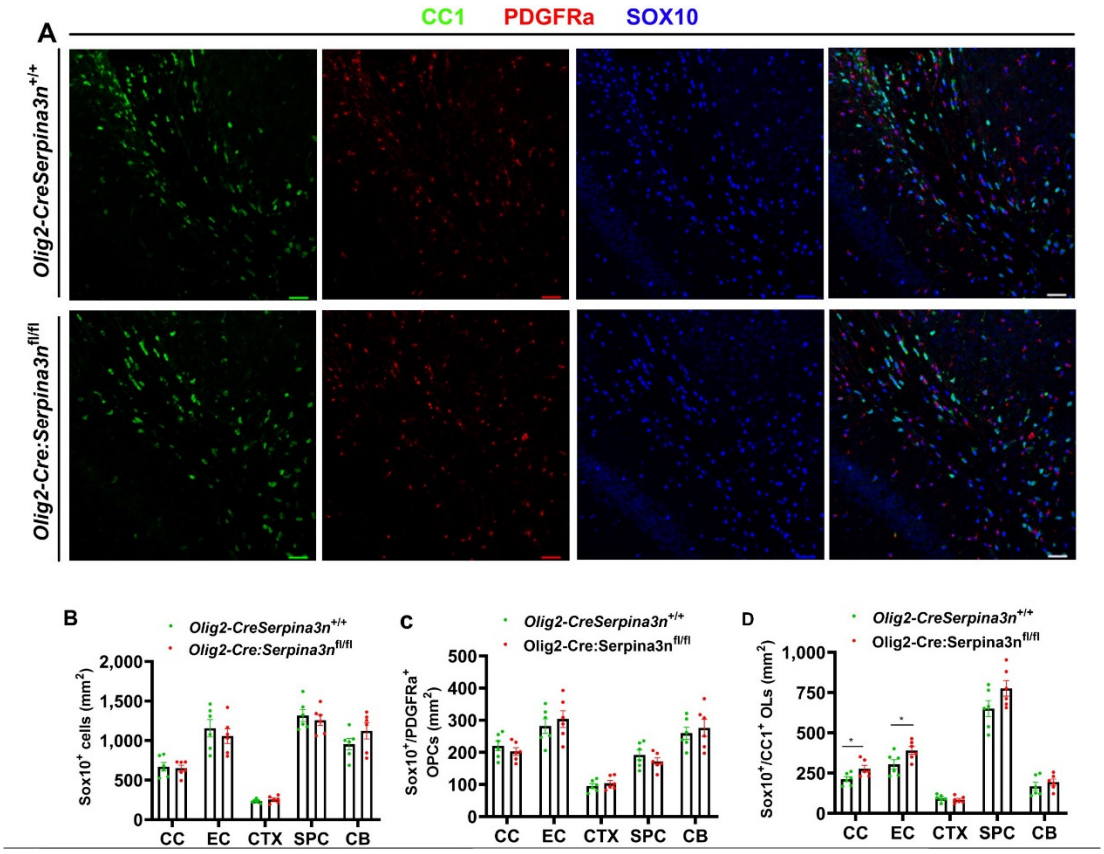

A, representative confocal images pan-oligodendroglial lineage marker SOX10, differentiated OL marker CC1, and OPC marker PDGFRa in the corpus callosum (CC). **B**, quantification of pan-oligodendroglial lineage cells in different regions of the CNS. Two-tailed Student's t test, CC t=0.2806, df=10 P=0.2847; external capsule (EC) *t*=0.6917, df=10 *P*=0.5048; cerebral cortex (CTX) *t*=0.9386, df=10 *P*=0.3701; spinal cord (SPC) *t*=0.5732, df=10 *P*=0.5792; cerebellum (CB) *t*=1.354, df=10 *P*=0.2055. **C**, quantification of OPCs. Two-tailed Student's t test, Sox10+/PDGFRa+: CC *t*=8958, df=10 *P*=0.3914; EC *t*=0.6342, df=10 *P*=0.5402; CTX *t*=0.7610, df=10 *P*=0.4642; SPC *t*=1.056, df=10 *P*=0.3156; CB *t*=0.5225, df=10 *P*=0.6127. **D**, quantification of OLs. Two-tailed Student's t test, Sox10+/CC1+: CC *t*=2.509, df=10 *P*=0.0310; EC *t*=2.303, df=10 *P*=0.0440; CTX *t*=0.7504, df=10 *P*=0.4703; SPC *t*=1.8010, df=10 *P*=0.1019; CB *t*=0.8010 df=10 *P*=0.4417. CNS tissues were harvested at P15. Scale bars = 50 µm

We next aimed to assess the rate of oligodendroglial differentiation in additional to the accumulative population of differentiated OLs (**Fig. 5**). To quantify oligodendroglial differentiation rate, we sought to TCF7l2, a nuclear marker labeling newly differentiated OLs and downregulation in mature OLs and reflecting the rate of oligodendrogenesis at any given time points (Guo et al., 2023). The nuclear expression of TCF7l2 makes quantification much easier than cell surface markers (**Fig. 6A**). No marked or statistically significant difference was observed in the densities of TCF7L2^{+} cells among different CNS areas (Fig. 6B), suggesting that Serpina3n deficiency did not affect the rate of oligodendrogenesis in vivo. Consistently, the

expression of myelin basic protein (MBP), one of the major structural proteins in myelin sheath, appeared to be comparable in most white matter tract of Serpina3n cKO and Ctrl mice (**Fig. 6A, C**).

Figure 6 – Serpina3n deficiency does not affect the rate of oligodendrocyte genesis during normal development.

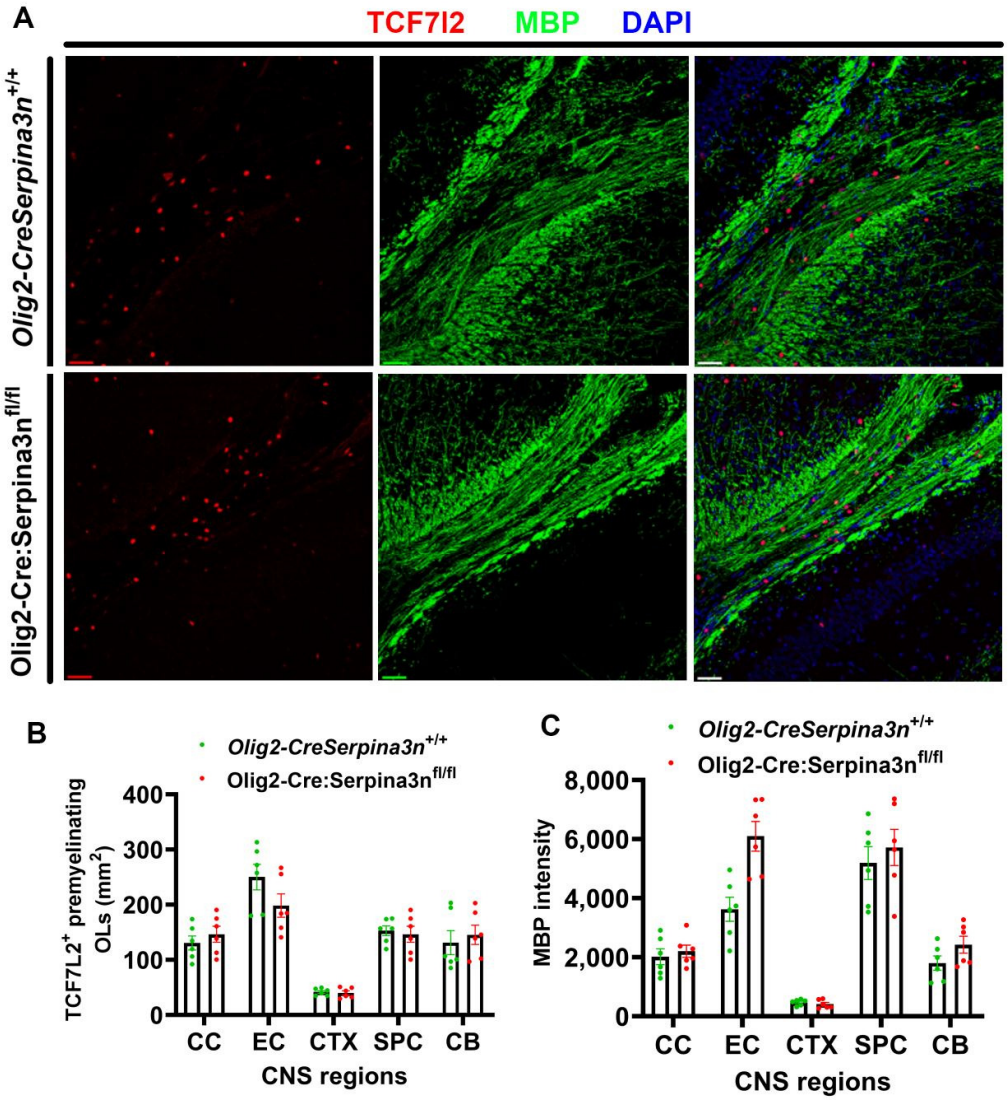

A, , representative confocal images of newly generated premyelinating OL marker TCF7l2 and myelin structure protein MBP in the CC. **B,** quantification of TCF7l2+ cells. Two-tailed Student's t test, TCF4: CC t=0.8234, df=10 P=0.4295; EC t=1.646, df=10 P=0.1309, CTX t=0.3702, df=10, P=0.7190; SPC: t=0.3770, df=10, P=0.7141. CB t=0.5059, df=10, P=0.6239. **C**, quantification of MBP intensity. Two-tailed Student's t test, CC t=5526, df=10, P=0.5927; EC t=3.807, df=10, P=0.0034; CTX t=0.8591, df=10, P=0.4104; SPC t=0.6395, df=10, P=0.5369; CB t=1.640, df=10, P=0.1320. CNS tissues were harvested at P15. Scale bars = 50 µm

To determine the potential cell-autonomous effects of Serpina3n on oligodendroglial differentiation, primary OPCs were isolated from the neonatal brain of Serpina3n cKO and Ctrl mice (**Fig. 7A**). Upon incubating primary OPCs in the differentiation medium, the generation of MBP^{+} OLs appeared indistinguishable between Serpina3n-deficient OPCs and -sufficient OPCs in the dish (**Fig. 7B**). Taken together, Serpina3n play a minor role, if any, in regulating oligodendroglial differentiation both in vivo and in vitro.

Figure 7 - Serpina3n deficiency does not affect the normal differentiation of OPCs into OLs in vitro (Meina, be prepared for an in-depth analysis using primary culture upon revision)

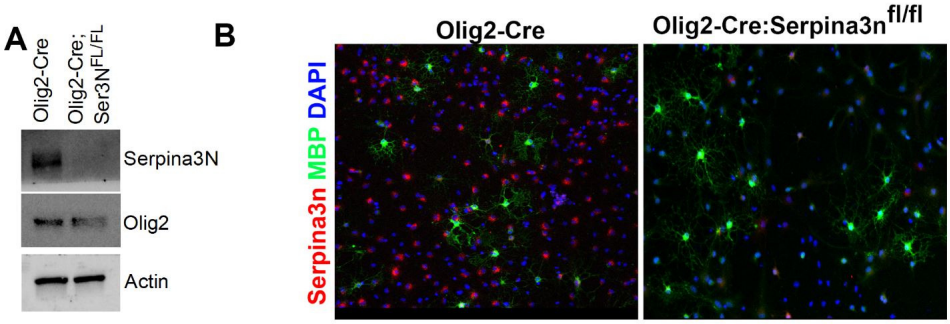

A, Western blot assay for Serpina3n in D2 primary oligodendrocyte culture derived from P1 Olig2-Cre and Olig2-Cre:Serpina3nfl/fl pups. **B**, fluorescent immunocytochemistry of Serpina3n and myelin basic protein MBP in D3 primary OLs.

4. Developmental myelination appears to proceed normally in Serpina3n-deficient mice

We next employed transmission electron microscopy (TEM) to assess potential myelination abnormalities at the ultrastructural level (**Fig. 8A**) (Yan et al., 2022). G-ratio, the ratio of inner axon diameter versus the total fiber diameter (inner axon and outer myelin) (**Fig. 8B, right**) was statistically comparable in Serpina3n-deficient mice to that in Ctrl mice (**Fig. 8B left, Fig. 8C**), suggesting that myelin sheath thickness of myelinated axons was unaffected by Serpina3n depletion. Furthermore, Serpina3n depletion did not alter the normal dynamics of axonal diameters (**Fig. 8D**) or the density of myelinated axons (**Fig. 8E**).

Figure 8 – normal myelination in Serpina3n cKO mice evaluated by transmission electron microscopy (TEM)

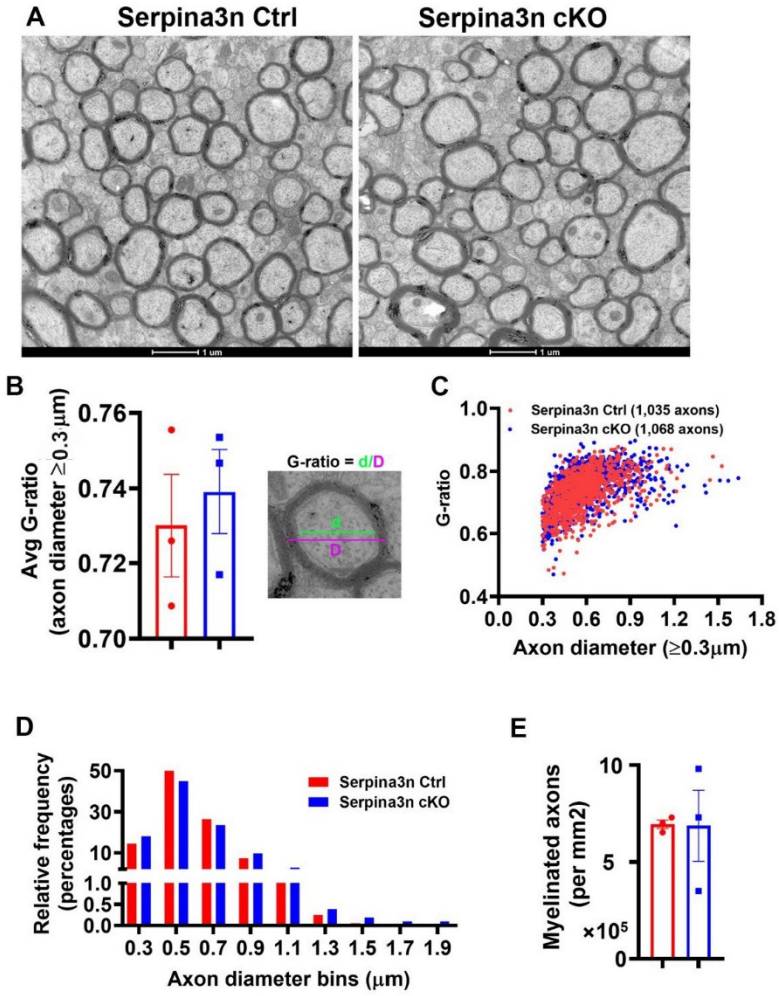

A, representative TEM images from the corpus callosum demonstrating indistinguishable myelination profiles between Serpina3n Ctrl and cKO mice. Scale bars=1µm. **B**, Average g-ratio of myelinated axons in the CC. Two-tailed Student's t test *t*=0.5105, df=4, *P*=0.6366. **C**, scatter plot of G-ratio and axon diameters of individual axons (≥0.3µm in diameter). **D**, axon diameter frequency distribution. **E**, densities of myelinated axons. Two-tailed Student's t test with Welch's correction *t*=0.0421, df=2.059 *P*=0.9702. The CNS tissues were harvested at P60.

5. Serpina3n deficiency does not perturb the normal development of astroglia, microglia or neurons

We reasoned that oligodendroglia-derived Serpina3n may regulate the development of other glial cells or neurons in a paracrine manner given its secretory nature. To this end, fluorescence IHC was used to quantify the population of astrocytes (GFAP) and microglia (Iba1) throughout

different CNS regions (**Fig. 9A**). Our systemic quantification failed to reveal any statistically significant differences in the number of GFAP⁺ astrocytes (**Fig. 9B**) or Iba1⁺ microglia (**Fig. 9C**).

Figure 9 – Serpina3n deficiency does not affect astroglial or microglial development

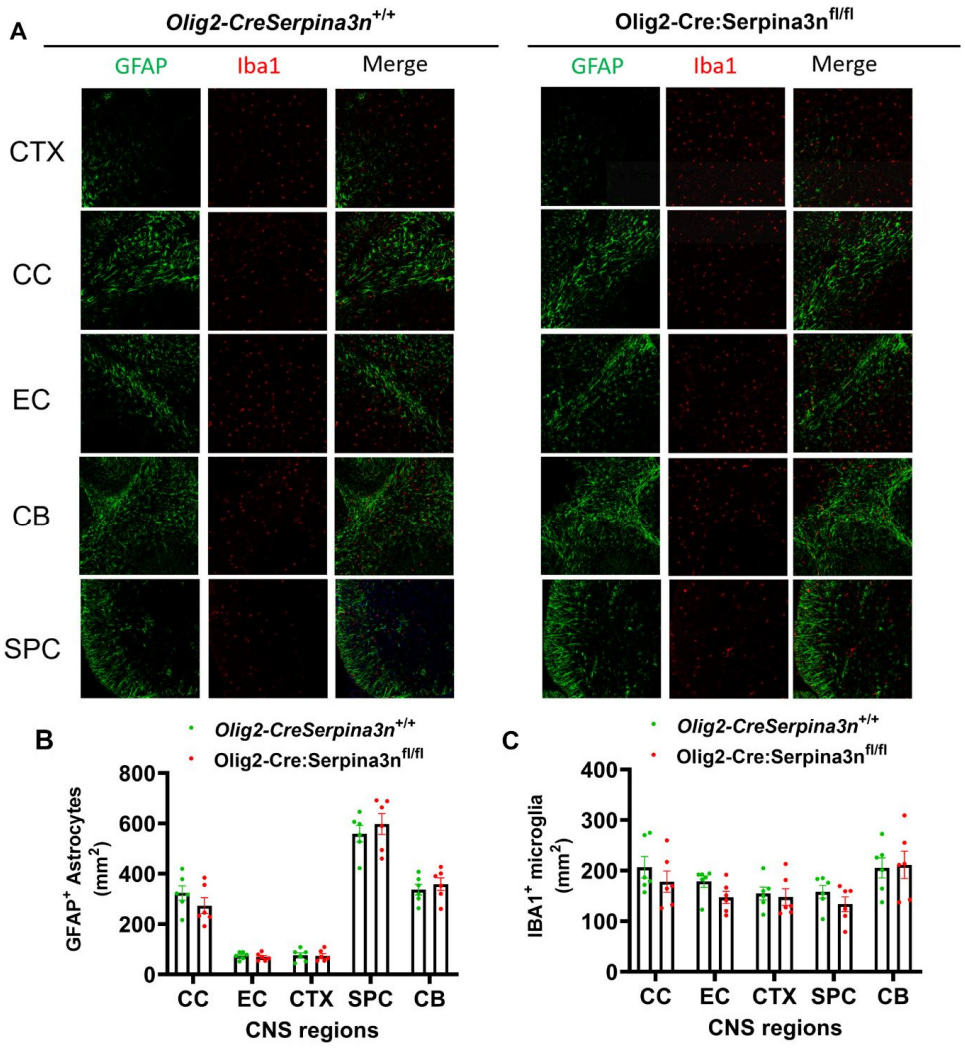

A, representative confocal images of astroglial marker GFAP and microglial marker IBA1 in different CNS regions. **B**, quantification of GFAP+ astrocytes. Two-tailed Student's t test, CC t=1.177, df=10 P=0.2663; EC t=0.6233, df=10 P=0.5740; CTX t=0.1433, df=10 P=0.8889; SPC t=0.7363, df=10 P=0.4785; CB t=0.6508, df=10 P=0.0.5299. **C**, quantification of IBA1+ parenchymal microglia. Two-tailed Student's t test, CC t=0.9514, df=10 P=0.3638; EC t=1.894, df=10 P=0.0875; CTX t=0.3510, df=10 P=0.7329; SPC t=1.271, df=10 P=0.2323; CB t=1.271, df=10 P=0.2329. CNS tissues were harvested at P15.

We next evaluate neuronal development in Serpina3n-deficient mice. IHC of NeuN, which labels neuronal cell bodies, and MAP2a, which labels neuronal dendrites and cell bodies, was used to quantify neuron population development (**Fig. 10A**). Our data showed that the

density of neurons in the cerebral cortex was unaffected by Serpina3n deficiency (**Fig. 10B**). Similar conclusion was drawn by MAP2a quantification (**Fig. 10C**). Taken together, these quantitative data suggest that oligodendroglia-derived Serpina3n is dispensable for normal development of other glial cells and neurons in the CNS.

Figure 10 – Normal neuronal development in Serpina3n cKO mice.

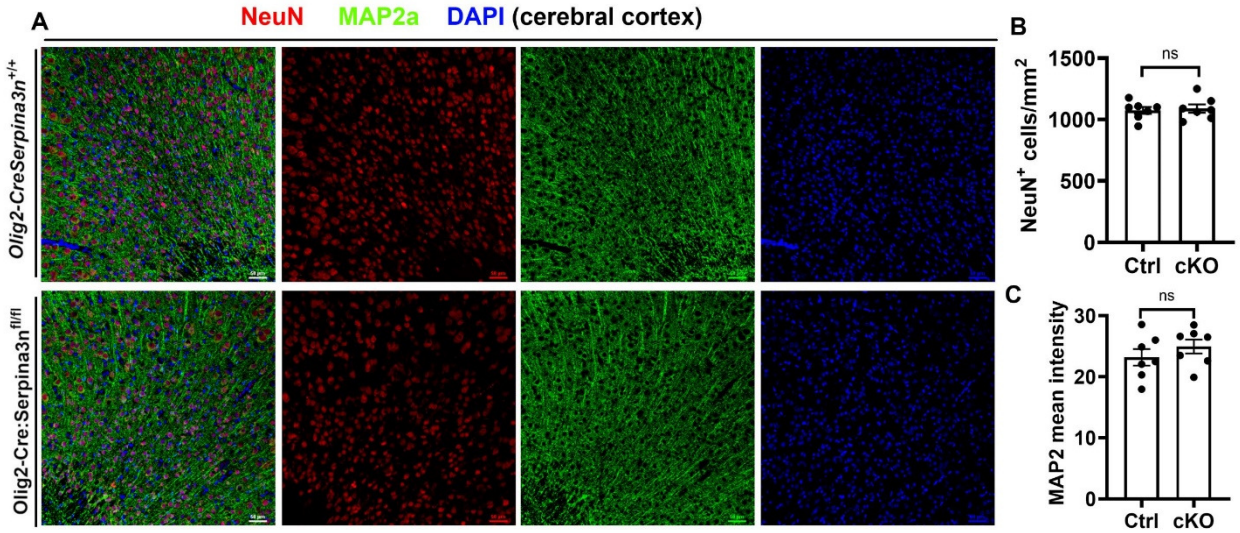

A, representative confocal images of neuronal cell body marker NeuN and neurite marker MAP2a in the brain cerebral cortex. **B-C**, quantification of NeuN$^+$ neuron population and MAP2a$^+$ intentisy. Student's t test, NeuN t=0.3359, df=12 P=0.7427; Map2a t=0.9995, df=12 P=0.3373. Brain collection at P15. Scale bars = 50 µm

6. Molecular changes of brain cells in Serpina3n-deficient and control mice

Having demonstrated that Serpina3n play a minor role in oligodendroglial myelination and brain development, we next sought to quantify potential molecular alterations in glial cells and neurons. For this purpose, magnetic-assisted cell soring (MACS) (Zhang *et al.*, 2021a) was employed to acutely isolate microglia (CD11b), oligodendroglia (O4), astrocytes (ACSA2), and brain remnant cells (containing all neurons) (**Fig. 11A**). RT-qPCR assay of lineage-specific marker genes demonstrated that MACS cells was highly purified populations with little contamination of other cell types: Tmem119 for microglia, Sox10 for oligodendroglia, Aldh1l1 for astroglia (**Fig. 11B**). Our RT-qPCR quantification of oligodendroglial mRNA showed no difference in the molecular expression of important functional genes of oligodendroglial development, such as *Sox10, Pdgfra*, and *Tcf7l2* (**Fig. 11C**) and a panel of genes coding myelin proteins (**Fig. 11D**). The expression level of astroglial signature genes (*Gfap*, *Aldh1l1*) and crucial functional genes (Slc1a2, Slc1a3, Aqp4) was comparable between Serpina3n cKO mice

and Ctrl mice (**Fig. 11E**). Moreover, microglial signature and functional genes was shown no difference in Serpina3n cKO mice compared to Ctrl mice (**Fig. 11F**). Because neurons were isolated into the triple negative cell component, we quantify neuronal marker genes (Map2a, Tubb3, Syp, NeuN) and found not difference in their mRNA expression between Serpina3n cKO and Ctrl mice (**Fig. 11G**). Altogether, these data of molecular assays suggest that Serpina3n plays a minor role, if any, in oligodendrocyte differentiation, myelination, and brain cell development.

Figure 11 - unperturbed molecular expression of glial and neurons in acutely isolated cells

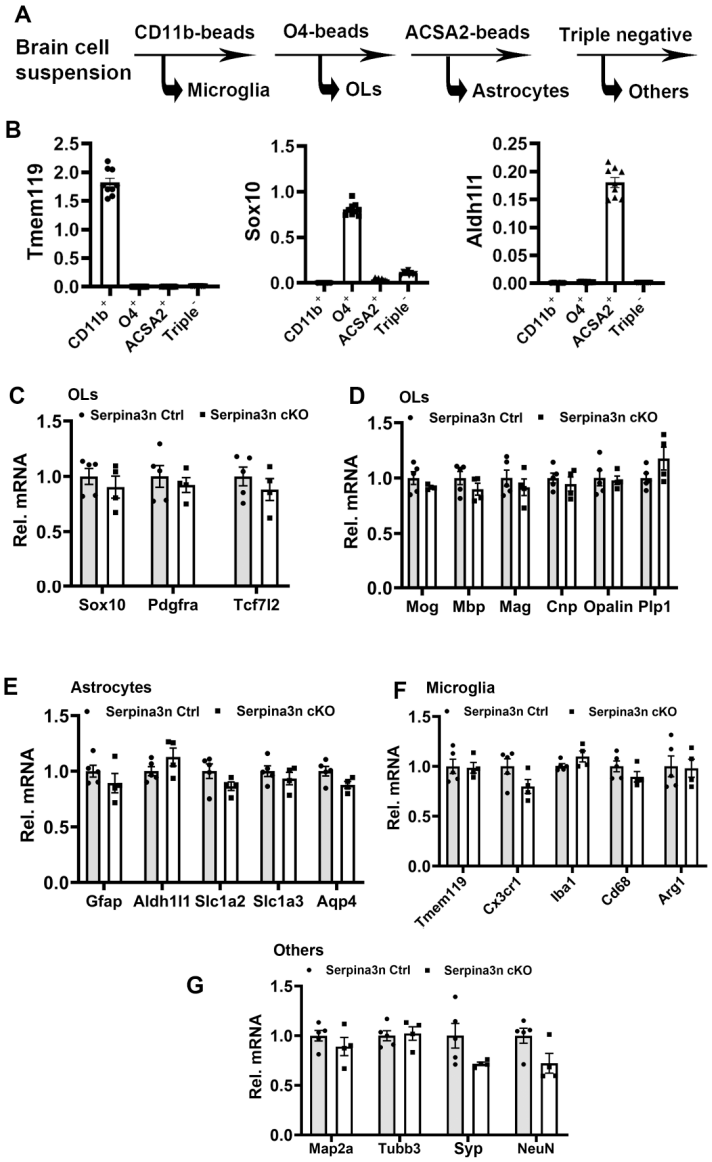

A, Experimental flowchart of acute isolation of CD11b$^+$ microglia, O4$^+$ OLs, ACSA2$^+$ astrocytes, and triple-negative other brain cells by magnetic-assisted cell sorting (MACS) from P12 mouse brains. **B**, purity assays (by RT-qPCR) of each cell populations by lineage-specific markers, Tmem119 for microglia, Sox10 for OLs, and Aldh1l1 for astrocytes. **C**, RT-qPCR assay for the key genes of oligodendroglial development and differentiation in MACS-purified OLs. Sox10 t=0.8067, df=7 P=0.4464; Pdgfra t=0.6150, df=7 P=0.5580; Tcf7l2 t=0.9178, df=7 P=0.3893. **D**, RT-qPCR assay for major oligodendroglial myelin-enriched genes in MACS-purified OLs. Mog t=1.242, df=7 P=0.2542; Mbp t=1.212, df=7 P=0.2645; Mag t=0.7946, df=7 P=0.4529; Cnp t=0.7261, df=7 P=0.4914; Opalin t=0.2423, df=7 P=0.8155; Plp1 t=1.721, df=7 P=0.1290. **E**, RT-qPCR assay for astrocyte marker genes in MACS-purified astrocytes. Gfap t=1.102, df=7 P=0.3068; Aldh1l1 t=1.509, df=7 P=0.1751; Slc1a2 t=1.662, df=7 P=0.1405; Slc1a3 t=0.9015, df=7 P=0.3973; Aqp4 t=2.210, df=7 P=0.0628. **F**, RT-qPCR assay for microglial marker genes in MACS-purified microglia. Tmem119 t=0.15352, df=7 P=0.8825; Cx3cr1 t=1.914, df=7 P=0.0972; Iba1 t=1.741, df=7 P=0.1251; Cd68 t=1.352, df=7 P=0.2185; Arg1 t=0.1326, df=7 P=0.8983. **G**, RT-qPCR assay for neuronal marker genes in triple-negative brain cells. Map2a t=1.080, df=7 P=0.3160; Tubb3 t=0.2726, df=7 P=0.7930; Syp t=2.003, df=7 P=0.0553; NeuN t=2.279, df=7 P=0.0567.

Discussion

SERPINA3/Serpina3n displays tissue-specific expression under homeostasis, primarily in the liver and the brain (www.proteinatlas.org/ENSG00000196136-SERPINA3/tissue, www.ncbi.nlm.nih.gov/gene/12) and plays diverse roles under physiological conditions. For example, loss-of-function variants in SERPINA3 gene were reported to associate with certain cancer susceptibility (Koivuluoma et al., 2021) and generalized pustular psoriasis (Ortega et al., 2010) (Frey et al., 2020) in certain populations. Furthermore, SERPINA3 is an established acute-phase response protein during inflammation, potentially fine-tuning immune activity. It is now increasingly recognized that the developing brain is an active component of the innate immune response (Herrera-Rincon et al., 2020; Lenz and Nelson, 2018; Zengeler and Lukens, 2021). It remains elusive if the immune-related protein SERPINA3/Serpina3 participates in normal brain development.

One of the significant findings of this study is that Serpina3n protein product was expressed primarily in oligodendroglia during early postnatal development of the murine CNS. Interestingly, it appears that Serpina3n mRNA level is not always correlated with its protein products (Fig. 1A vs Fig. 1B). We also observed the uncorrelation of Serpina3n mRNA versus protein in acutely isolated brain cells (Fig. 11A-B); the mRNA level of Serpina3n in acutely isolated astrocytes is about 10-fold higher than that in oligodendrocytes in the developing brain quantified by RT-qPCR (data not shown). Yet, our IHC data clearly demonstrated that Serpina3n protein was primarily located in oligodendrocytes, which was validated by Serpina3n genetic knockout study (Fig. 2). A previous genomic study reported that Serpina3n mRNA was a lineage specific marker of reactive astrocytes in response to lipopolysaccharide (LPS)-induced

neuroinflammation and ischemia stroke (Zamanian *et al.*, 2012). However, that study did not evaluate the expression of Serpina3n protein in the brain. In our unpublished study, we employed the same LPS injection protocol as reported by Zamanian et al., 2012 and surprisingly fount that Serpina3n protein is expressed primarily by Sox10+ oligodendroglia but not by GFAP+ reactive astrocytes, which suggests that Serpina3n protein level does not necessarily correlated with its transcript. To further support this idea, a public RNA and protein expression database shows that SERPINA3 protein level is much higher in the brain than that in the liver, yet the mRNA level shows the opposite (www.proteinatlas.org/ENSG00000196136-SERPINA3/tissue). At the protein level, we also found that, in additional to oligodendroglia, a restricted subpopulation of neurons in the basal-lateral nuclei of hypothalamus around the third brain ventricle displays high level of Serpina3n protein (data not shown), which is consistent with previous reports (Dalby et al., 2018; Sergi et al., 2018). The biological mechanism and significance of differential regulation of Serpina3n protein from its transcript in oligodendroglia versus astroglia warrants further studies.

The physiological role of SERPINA3/Serpina3n in murine CNS development remains an open question. A recent study attempted to answer this question by using gain-of-function approaches (Zhao *et al.*, 2022). It was reported that SERPINA3 was expressed in neural precursor cells (radial glia) of the human embryonic brain and that SERPINA3 increased radial glia pool and neurogenesis, and impressively, augmented cognitive function when ectopically over-expressed in mice (Zhao *et al.*, 2022). These data suggest a crucial role of human SERPINA3 in neurogenesis and cognition under homeostasis. It would be important and necessary to employ brain-specific loss-of-function approaches to confirm if Serpina3n ablation affects neurogenesis and impact mouse cognitive behavior.

Because of Serpina3n expression in oligodendroglial lineage cells during early postnatal CNS development, we employed oligodendroglia-specific ablation to investigate its physiological role in oligodendroglial myelination and animal behaviors. Serpina3n cKO mice did not show ataxia or tremor, which is the typical motor function manifestation of CNS developmental hypomyelination; their motor coordination, motor learning ability, regularity index of walking gait, and spatial learning and memory were all unaltered compared to the control animals. We noticed that Serpina3n cKO mice display impaired cognitive ability during the initial training trials (Fig. 4A) yet behave indistinguishably during the subsequent training and test trials to their controls. Consistently, our thorough analyses at the histological and molecular levels demonstrated overall comparable rates of oligodendrocyte differentiation, myelination, microglial/astroglial and neuronal development in Serpina3n cKO mice to those in control mice.

Based on these data, we conclude that Serpina3n plays a minor role, if any, in regulating oligodendroglial myelination, brain cell development and animal motor/cognitive function under homeostasis.

The research interest of SERPINA3/Serpina3n under neurological conditions was initially sparked by the discovery of its pathological accumulation in the amyloid deposits of Alzheimer's brain (Abraham et al., 1988) and normal ageing brain (Abraham and Potter, 1989a; b) and further ignited by the recent discovery that Serpina3n is one of the top signature genes of a population of oligodendrocytes, disease-associated oligodendrocytes, among various neuropathies including normal ageing (Kenigsbuch *et al.*, 2022). Our data showed that Serpina3n was significantly upregulated and secreted out of oligodendrocytes in response to oxidative stress/injury (**Fig. 1**), a common pathological feature existing in various neurological conditions including normal ageing (Allen and Bayraktutan, 2009; Chen et al., 2012; Fesharaki-Zadeh, 2022; Liguori et al., 2018; Ljubisavljevic, 2016). Further studies are needed to probe the potential role of injury-responsive molecule Serpina3n in regulating neurological disease pathogenesis. The genetic mouse lines of the current study provide powerful tools for answering these questions.

Materials and Methods:

Transgenic mice `

All mice were housed at 12 h light/dark cycle with free access to food and drink, and both males and females were used in this study. All transgenic mice were maintained on a C57BL/6 background and approved by Institutional Animal Care and Use Committee at the University of California, Davis. B6.129-Olig2tm1.1(cre)Wdr/J (Olig2-cre, RRID:IMSR_JAX:025567) (Schuller et al., 2008) and B6.129S-Serpina3ntm1.1Lbrl/J (Serpina3nfl/fl, RRID:IMSR_JAX:027511) mice (Vicuna *et al.*, 2015) were purchased from JAX. Animal genotype was determined by PCR of genomic DNA extracted from tail tissue. All Cre lines were maintained as heterozygosity.

Tissue harvesting and processing

Serpina3n cKO mice and Ctrl mice were anesthetized by ketamine (150 mg/kg)/xylazine (15 mg/kg) mixture and transcardially perfused with ice-cold PBS. Harvested brain and spinal cord were placed immediately on dry ice for protein or RNA extraction or fixed in fresh 4% paraformaldehyde (PFA) in 0.1 m PBS overnight at 4°C for histological study. Then tissues were

washed with PBS three times, 30 min per time and cryopreserved in 30% sucrose in PBS overnight at 4°C followed by embedding in O.C.T. (Cat# 361603E, VWR International). Serial sections (12 μm) were cut using a Leica Cryostat (CM1900-3-1). All slides were stored in –80°C freezers.

Immunohistochemistry (IHC)

Sections were air-dried for 2 h and blocked in 10% donkey serum in 0.1% PBS Tween 20 (PBST) for 2 h at room temperature. For Serpina3n staining, slides were fixed with 100% methanol for 10 minutes at -20°C. Sections were washed with 0.1% PBST and incubated in primary antibody. After three times washing with PBST, slices were incubated with secondary antibodies for 2 h at room temperature. DAPI was used as a nuclear counterstain. Images were taken using a Nikon A1 confocal microscope. A z-stack of optical sections, 10 μm in total thickness, were collapsed into a single 2D image for quantification. The following antibodies were used for our IHC study: Goat anti-Serpina3n (1:3000, R&D System, Cat# AF4709, RRID:AB_2270116); Mouse anti-CC-1 (1:100, Millipore, Cat# OP80, RRID:AB_2057371); Goat anti-PDGFRα (1:200, R&D System, Cat# AF1062, RRID:AB_2236897); Rabbit anti-Sox10 (1:200, Abcam, Cat# ab155279, RRID:AB_2650603); Rabbit anti-TCF4/TCF7L2 (1:200, Cell Signaling Technology, Cat# 2569, RRID:AB_2199816); Mouse anti-MBP (1:200, MilliporeSigma, Cat# NE1019, RRID:AB_2140491); Mouse anti-GFAP (1:1000, Millipore, Cat# MAB360, RRID:AB_11212597); Rabbit anti-Iba1 (1:500, WAKO, Cat# 019-19741, RRID:AB_839504); Mouse anti-NeuN (1:500, Millipore, Cat# MAB377, RRID:AB_2298772). The signal was visualized by a secondary antibody Alexa Fluor 488- or Alexa Fluor 594-conjugated AffiniPure F(ab')2 fragments (1:400, Jackson ImmunoResearch).

Primary oligodendrocyte culture

Primary oligodendrocyte cultures were established following a previously outlined protocol (Zhang et al., 2021b). Pups, aged P2, were dissected in ice-cold HBSS (#24020117, Thermo Fisher) under a microscope. Isolated tissues underwent dissociation using a papain dissociation kit (#LK003176, Worthington) supplemented with DNase I (250 U/ml; #D5025, Sigma) and D-(+)-glucose (0.36%; #0188 AMRESCO) at in 37 ℃/5% CO_2 for 60 min. Tissue chunks were then transferred to the PDS Kit-Inhibitor solution (#LK003182, Worthington) and filtered through strainers. After centrifugation, the cell suspension was transferred to a poly-D-lysine (PDL, #A003-E, Millipore) pre-coated T-75 flask and maintained in DMEM/F12 (#11320033, Gibco) containing heat-inactivated fetal bovine serum (#12306-C, Sigma) and 1%

penicillin/streptomycin (P/S, #15140122, Gibco) at in 37 ℃/5% CO2 . The medium was replaced 50% every other day. When cells reached confluency around 11-14 days, the shaking method was applied to detach cells. To collect OPCs, microglia were detached with 220 rpm shaking for 2 hours at 37 ℃, and the supernatant was removed. 20 ml of serum-free growth medium (GM), a 3:7 mixture (v/v) of B104 neuroblastoma-conditioned medium, 10 ng/ml biotin (#B4639, Sigma), and N1 medium (high-glucose DMEM supplemented with 5 μg/ml insulin (#I6634, Sigma), 50 μg/ml apo-transferrin (#T2036, Sigma), 100 μM putrescine (#P5780, Sigma), 30 nM Sodium selenite (#S5261, Sigma), 20 nM progesterone (#P0130, Sigma) was added to each flask and shaken at 220 rpm for 6 hours. The supernatant was then collected into a 50 ml tube and centrifuged at 1800 rpm for 5 minutes. OPCs were cultured on PDL-coated plates with complete GM, consisting of GM with 5 ng/ml FGF (#450-33, Peprotech), 4 ng/ml PDGF-AA (#315-17, Peprotech), 50 □M forskolin (#6652995, Peprotech), and glutamax (#35050, Thermo Fisher). To induce differentiation, the medium was switched to differentiation medium (DM), composed of 12.5 μg/ml Insulin, 100 μM Putrescine, 24 nM Sodium selenite, 10 nM Progesterone, 10 ng/ml Biotin, 50 μg/ml Transferrin (#T8158, Sigma), 30 ng/ml 3,3′,5-Triiodo-L-thyronine (#T5516, Sigma), 40 ng/ml L-Thyroxine (#T0397, Sigma-Aldrich), glutamax, and P/S in F12/high-glucose DMEM, 1:1 in medium (#11330032, Thermo Fisher Scientific). After 3 days of differentiation, OLs were treated with PBS or 50 mM or 200 mM H_2O_2.

Enzyme-linked immune sorbent assay (ELISA) of Serpina3n

The medium collected from primary culture were used for Serpina3n measurement assay at day 3 of differentiation. The Serpina3n concentration was determined using the mouse Serpina3n ELISA kit (BIOMATIK, EKF58884). ELISA was performed according to the manufacturer's instruction.

Magnetic-activated cell sorting (MACS)

Single-cell suspensions were prepared following the instructions provided by Miltenyi Biotec. Mouse brains from Control and Serpina3n cKO mice were processed using the Neural Tissue Dissociation Kit (P) (Cat# 130-092-628, Miltenyi Biotec, Germany) in conjunction with the gentleMACS Dissociator (Cat# 130-093-235, Miltenyi Biotec, Germany). The mouse brains were collected, cut into 0.5 cm pieces using a scalpel, and transferred into a pre-heated gentleMACS C tube (Cat# 130-093-237, Miltenyi Biotec, Germany). Enzymatic cell dissociation was initiated using 1950 μL of Enzyme mix 1 (Enzyme P and Buffer X). The C tube was attached upside down onto the sleeve of the gentleMACS Dissociator, and the brain tissue was dissociated

using the appropriate gentleMACS program. After one rotation, 30 µL of enzyme mix 2 (Enzyme A and Buffer Y) was added into the C Tube, followed by two gentle rotations at 37°C. Upon program completion, the C Tube was detached, briefly centrifuged, and the sample at the bottom of the tube was filtered through a MACS SmartStrainer (70 µm) to remove cell clumps, achieving a single-cell suspension. The MACS SmartStrainer was washed with an additional 10 mL of HBSS (w) (HBSS with Ca2+ and Mg2+, Cat# 55021C, Sigma-Aldrich) to collect all the cells. After centrifugation, the supernatant was gently removed, and the brain homogenate pellet was incubated separately with Anti-CD11b Microbeads (130-093-634, Miltenyi Biotec, Germany) and Anti-O4 Microbeads (130-094-543, Miltenyi Biotec, Germany), with Fc receptors blocking prior to Anti-ACSA-2 MicroBeads (Cat# 130-097-678, Miltenyi Biotec, Germany). Incubation was carried out for 15 minutes in the refrigerator at 4℃. Cells were washed with 0.5% BSA/PBS buffer and centrifuged at 300 g for 10 min. The supernatant was aspirated completely, and the cell pellet was resuspended in 500 µL of 0.5% BSA/PBS buffer before proceeding to magnetic separation.

The LS MACS column was positioned in the magnetic field of a MACS Separator (Cat#130-090-976, Miltenyi Biotec) and rinsed with 3 mL of 0.5% BSA/PBS buffer. The cell suspension was applied to the MS column, and the column was washed 3 times with 3 mL of 0.5% BSA/PBS buffer. Unlabeled cells were collected and combined with the flow-through. Magnetically labeled cells were immediately flushed out by firmly pushing the plunger into the column. Subsequently, 350 µL of Buffer RLT Plus containing β-mercaptoethanol (β-ME) was added to the cells, and the mixture was stored in a –80°C refrigerator.

RNA extraction, cDNA preparation, and RT-qPCR

RNA isolation was carried out using the RNeasy Plus Micro Kit (Cat#74034, QIAGEN) following the manufacturer's protocol. Harvested cells were transferred to a 1.5 ml tube and vortexed for 20 seconds. The lysate was then transferred to a gDNA Eliminator spin column placed in a collection tube. After centrifugation, 1 volume of 70% ethanol was added to the flow-through, mixed well by pipetting, and immediately transferred to an RNeasy MinElute spin column placed in a collection tube. The RNeasy MinElute spin column was washed with Buffer RW1, Buffer RPE, and 80% ethanol, and the collection tube with the flow-through was discarded. RNase-free water was added to the spin column membrane and centrifuged for 2 minutes at 14,000 rpm to elute the RNA. The RNA concentration and purity (260/280 and 260/230 ratios) were analyzed using a Nanodrop 2000 Spectrophotometer (Thermo Fisher Scientific).

For cDNA synthesis, 200 ng of total RNA was reverse-transcribed using the QIAGEN Omniscript RT Kit (Cat#205111, QIAGEN) according to the manufacturer's guidelines. The cDNA amplification was performed with a QuantiTect SYBR Green PCR Kit (Cat#204145, QIAGEN). Real-time PCR reactions were carried out and analyzed using an Agilent MP3005P thermocycler. For quantification, the mRNA expression level of target genes in each sample was normalized to that of Hsp90 as a reference gene. The fold change in gene expression level was calculated based on the equation 2^(Ct [cycle threshold][Hsp90] - Ct [target gene]). Primer sets were obtained from Integrated DNA Technologies.

RT-qPCR primers:

Gene name	Forward primer sequence	Reverse primer sequence
Sox10	ACACCTTGGGACACGGTTTTC	TAGGTCTTGTTCCTCGGCCAT
Pdgfrα	GAGAACAACGGAGGAGC	GCTGAGGACCAGAAAGACC
Mag	CTGCCGCTGTTTTGGATAATGA	AAGTCGAAACGGCATCGGGG
Mog	AGCTGCTTCCTCTCCCTTCTC	ACTAAAGCCCGGATGGGATAC
Plp1	GTTCCAGAGGCCAACATCAAG	CTTGTCGGGATGTCCTAGCC
Tcf7l2-E1	GGAGGAGAAGAACTCGGAAAA	ATCGGAGGAGCTGTTTTGATT
Gfap	GTGTCAGAAGGCCACCTCAAG	CGAGTCCTTAATGACCTCACCAT
Cnp	TTTACCCGCAAAAGCCACACA	CACCGTGTCCTCATCTTGAAG
Aldh1l1	AGCCACCTATGAGGGCATTC	TGAGTGTCGAGTTGAAAAACGTC
Cd68	TGTCTGATCTTGCTAGGACCG	GAGAGTAACGGCCTTTTTGTGA
Vim	GAGGAGATGAGGGAGTTGCG	CTGCAATTTTTCTCGCAGCC
Hsp90	AAACAAGGAGATTTTCCTCCGC	CCGTCAGGCTCTCATATCGAAT
Mbp	GGCGGTGACAGACTCCAAG	GAAGCTCGTCGGACTCTGAG
Myrf	CAGACCCAGGTGCTACAC	TCCTGCTTGATCATTCCGTTC
Serpina3	GCCTCGTCAGGCCAAAAAG	TGAACGTGTCAAGAGGGTCAA
Opalin	CTGCCTCTCACTCAACATCA	GCTGGATCAAAGTAAACAGC
Aqp4	ATCAGCATCGCTAAGTCCGTC	GAGGTGTGACCAGGTAGAGGA
Slc1a2	CAACGGAGGATATCAGTCTGC	TGTTGGGAGTCAATGGTGTC
Slc1a3	CAAGACACTGACACGCAAGGAC	CTTAACATCTTCCTTGGTGAGGC
Arg1	TTGGGTGGATGCTCACACTG	GTACACGATGTCTTTGGCAGA
Nfe2l2(Nrf2)	AACAGAACGGCCCTAAAGCA	GGGGTTCACGCATAGGAGCA
Hmox1	AAGCCGAGAATGCTGAGTTCA	GCCGTGTAGATATGGTACAAGGA
C1qA	CGGAATTCGACAAGGTCCTCACCAACCAG	CGGGATCCGGGGTCCTTCTCGATCC
Tmem119	CCTACTCTGTGTCACTCCCG	CACGTACTGCCGGAAGAAATC
p21	TCTTGCACTCTGGTGTCTGA	CTGCGCTTGGAGTGATAGAA

p16	CGTACCCCGATTCAGGTG	ACCAGCGTGTCCAGGAAG
Cx3cr1	GAGTATGACGATTCTGCTGAGG	CAGACCGAACGTGAAGACGAG
Map2a	GCCAGCCTCGGAACAAACA	GCTCAGCGAATGAGGAAGGA
Tubb3	TAGACCCCAGCGGCAACTAT	GTTCCAGGTTCCAAGTCCACC
Syp	CAGTTCCGGGTGGTCAAGG	ACTCTCCGTCTTGTTGGCAC
NeuN	ATCGTAGAGGGACGGAAAATTGA	GTTCCCAGGCTTCTTATTGGTC

Protein extraction and Western blot

Frozen tissues were homogenized in ice-cold N-PER Neuronal Protein Extraction Reagent (Thermo Fisher) containing protease inhibitor and phosphatase inhibitor cocktail (Cat# PPC1010, Thermo Fisher) and PMSF (Cat# 8553, Cell Signaling Technology) for 30 min and centrifuged at 14,000 rpm for 10 min at 4°C. Supernatants were collected and protein concentrations were measured using BCA protein assay Kit (Cat# 23225, ThermoFisher Scientific). Equal amounts of protein (30 μg) from each sample were loaded into SDS-PAGE gels (BIO-RAD) for electrophoresis. The proteins were transferred onto a 0.2 μm nitrocellulose membrane (Cat# 1704158, BIO-RAD) using Trans-blot Turbo Transfer system (Cat# 1704150, Bio-Rad). The membrane was then blocked in 5% BSA for 1 h at room temperature, and incubated with primary antibodies overnight at 4℃ with Mouse anti-β-actin (1:1000, Cell Signaling Technology, cat#3700),Goat anti-SerpinA3N (1:500, R&D Systems, AF7409), Goat anti-Olig2 (1:500, Novus Biologicals, Cat# AF2418). After three times of 10 min wash in PBST, membranes were incubated with horseradish peroxidase (HRP)-linked donkey anti-goat or donkey anti-mouse antibody. The membrane was imaged using Western Lightening Plus ECL (Cat# NEL 103001EA, PerkinElmer). The intensities of the bands were quantified by ImageJ software to analyzing the scanned grayscale value.

Transmission electron microscopy (TEM) for assessment of mylelination

Mice were anesthetized with ketamine/xylazine mixture and perfused with 4% PFA, followed by 60 mL 3% glutaraldehyde (Electron Microscopy Science, dilute in PBS, pH 7.4) at a speed of 5 mL per minute. The brain was carefully dissected and fixed with 3% glutaraldehyde overnight. Subsequently, the brain underwent 2 washes with 0.2 M sodium cacodylate buffer (pH 7.2, Electron Microscopy Science), each lasting 10 minutes, followed by post-fixation with 2% (w/v) aqueous osmium tetroxide (Electron Microscopy Science) for 2 hours. After two additional washes with sodium cacodylate (10 minutes each), the brain was dehydrated using a gradient of ethanol (50%, 70%, 90%, and 100%), followed by 3 washes with propylene oxide (30 minutes

each). The specimen was then incubated overnight in a 1:1 mixture of Propylene Oxide:Eponate Resin (Electron Microscopy Science) and subsequently treated with a 1:3 mixture of Propylene Oxide:Eponate Resin for 10 hours, followed by an overnight incubation in 100% Eponate Resin. The resulting specimens were embedded in EMBed-812 Resin for 2 days at 65℃.

Semithin sections (500 nm) were cut using a Leica EM UC6 microtome and incubated with 2% toluidine blue (Cat#194541, Ted Pella Inc.) at 100℃ for 2 minutes. These sections were then imaged using an Olympus BX61 microscope. Ultrathin sections (70–80 nm) were cut on a Leica EM UC7 microtome, collected on 1 mm Formvar-coated copper slot grids, double-stained with uranyl acetate and lead citrate, and imaged on a CM120 electron microscope.

Animal Behavior assessment Animals were acclimated to the behavioral room for a 30 minutes before the tests. 12-week-old Serpina3n cKO and control mice underwent motor skill assessments using the CatWalk and Rotarod, followed by the Barnes maze cognition test.

Accelerating Rotarod Test: The accelerating Rotarod test assessed animal motor coordination and performance according to established protocols. The Rotarod initiated at 4 rpm and accelerated to a maximum speed of 40 rpm, with a 1.2 rpm increment every 10 seconds. Mice underwent two consecutive days of training (four trials each day with a 60-minute interval between trials), followed by data collection on the subsequent day. Each trial had a maximum duration of 300 seconds, and the time spent on the rod and maximal falling speed were recorded and averaged over the four trials.

Noldus CatWalk Gait Analysis: Gait analysis was performed using the real-time video-tracked CatWalk XT system (Noldus Information Technology) within a walkway measuring 68 x 29 x 52.5 inches. Each animal underwent 3 runs in a day as a test session. Data collection parameters included a camera gain set to 20 and a detection threshold of 0.1, as per the manufacturer's instructions. Successful runs were defined as those occurring within 0.50 to 5.00 seconds, and the average of three successful runs was used for data analysis.

Barnes Maze Test: Spatial learning/memory and locomotion were evaluated using the Barnes maze. Mice were placed in the center of the maze (100 cm diameter) with twenty holes (10 cm diameter), aiming to locate the escaping (goal) box. The tests were conducted in a noise-free room with strong illumination (>300 LUX) and visual cues. Training spanned five consecutive days, with formal testing on day 6. Each animal underwent two trials per day with

an approximately 60-minute interval. The maximal trial duration was 5 minutes, unless the mice found the goal box. Ethovision XT.14 software monitored and recorded various parameters, including total errors before entering the escape box, latency to entering the goal box, total distance traveled (path length), and moving velocity on the maze.

Quantification of marker-positive cells

Quantification was performed by observers blind to genotype and treatment. The data graphing and statistical analyses were performed using GraphPad Prism (version 8.0, www.graphpad.com). Data were presented as mean ± SEM in this study. Scatter dot plots were used to quantify data throughout our manuscript. Each dot in the scatter dot plots represents one mouse or one independent experiment. Unpaired two-tailed Student's t test was used for statistically analyzing two groups of data and degree of freedom (df) were presented as t(df) in figure legends. Comparisons between more than two groups were analyzed by One-way ANOVA followed by Tukey's post-test. Shapiro-Wilk approach determined data normality. F test and Browne-Forsythe test were used to test variance equality of two groups and three or more groups, respectively. The p-value was defined as $*p < 0.05$, $**p < 0.01$, $***p < 0.001$, ns, not significant $p > 0.05$.

Reference

Abraham, C.R., and Potter, H. (1989a). Alpha 1-antichymotrypsin in brain aging and disease. Prog Clin Biol Res *317*, 1037-1048.

Abraham, C.R., and Potter, H. (1989b). The protease inhibitor, alpha 1-antichymotrypsin, is a component of the brain amyloid deposits in normal aging and Alzheimer's disease. Ann Med *21*, 77-81. 10.3109/07853898909149188.

Abraham, C.R., Selkoe, D.J., and Potter, H. (1988). Immunochemical identification of the serine protease inhibitor alpha 1-antichymotrypsin in the brain amyloid deposits of Alzheimer's disease. Cell *52*, 487-501. 10.1016/0092-8674(88)90462-x.

Allen, C.L., and Bayraktutan, U. (2009). Oxidative stress and its role in the pathogenesis of ischaemic stroke. Int J Stroke *4*, 461-470. 10.1111/j.1747-4949.2009.00387.x.

Chen, X., Guo, C., and Kong, J. (2012). Oxidative stress in neurodegenerative diseases. Neural regeneration research *7*, 376-385. 10.3969/j.issn.1673-5374.2012.05.009.

Dalby, M.J., Aviello, G., Ross, A.W., Walker, A.W., Barrett, P., and Morgan, P.J. (2018). Diet induced obesity is independent of metabolic endotoxemia and TLR4 signalling, but markedly increases hypothalamic expression of the acute phase protein, SerpinA3N. Sci Rep *8*, 15648. 10.1038/s41598-018-33928-4.

de Mezer, M., Rogalinski, J., Przewozny, S., Chojnicki, M., Niepolski, L., Sobieska, M., and Przystanska, A. (2023). SERPINA3: Stimulator or Inhibitor of Pathological Changes. Biomedicines *11*. 10.3390/biomedicines11010156.

DeKosky, S.T., Ikonomovic, M.D., Wang, X., Farlow, M., Wisniewski, S., Lopez, O.L., Becker, J.T., Saxton, J., Klunk, W.E., Sweet, R., et al. (2003). Plasma and cerebrospinal fluid alpha1-antichymotrypsin levels in Alzheimer's disease: correlation with cognitive impairment. Ann Neurol *53*, 81-90. 10.1002/ana.10414.

Fesharaki-Zadeh, A. (2022). Oxidative Stress in Traumatic Brain Injury. Int J Mol Sci *23*. 10.3390/ijms232113000.

Fissolo, N., Matute-Blanch, C., Osman, M., Costa, C., Pinteac, R., Miro, B., Sanchez, A., Brito, V., Dujmovic, I., Voortman, M., et al. (2021). CSF SERPINA3 Levels Are Elevated in Patients With Progressive MS. Neurol Neuroimmunol Neuroinflamm *8*. 10.1212/NXI.0000000000000941.

Frey, S., Sticht, H., Wilsmann-Theis, D., Gerschutz, A., Wolf, K., Lohr, S., Haskamp, S., Frey, B., Hahn, M., Ekici, A.B., et al. (2020). Rare Loss-of-Function Mutation in SERPINA3 in Generalized Pustular Psoriasis. J Invest Dermatol *140*, 1451-1455 e1413. 10.1016/j.jid.2019.11.024.

Herrera-Rincon, C., Pare, J.F., Martyniuk, C.J., Jannetty, S.K., Harrison, C., Fischer, A., Dinis, A., Keshari, V., Novak, R., and Levin, M. (2020). An in vivo brain-bacteria interface: the developing brain as a key regulator of innate immunity. NPJ Regen Med *5*, 2. 10.1038/s41536-020-0087-2.

Horvath, A.J., Irving, J.A., Rossjohn, J., Law, R.H., Bottomley, S.P., Quinsey, N.S., Pike, R.N., Coughlin, P.B., and Whisstock, J.C. (2005). The murine orthologue of human antichymotrypsin: a structural paradigm for clade A3 serpins. J Biol Chem *280*, 43168-43178. 10.1074/jbc.M505598200.

Jain, S., Gautam, V., and Naseem, S. (2011). Acute-phase proteins: As diagnostic tool. J Pharm Bioallied Sci *3*, 118-127. 10.4103/0975-7406.76489.

Kenigsbuch, M., Bost, P., Halevi, S., Chang, Y., Chen, S., Ma, Q., Hajbi, R., Schwikowski, B., Bodenmiller, B., Fu, H., et al. (2022). A shared disease-associated oligodendrocyte signature among multiple CNS pathologies. Nat Neurosci *25*, 876-886. 10.1038/s41593-022-01104-7.

Ko, E., Kim, J.S., Bae, J.W., Kim, J., Park, S.G., and Jung, G. (2019). SERPINA3 is a key modulator of HNRNP-K transcriptional activity against oxidative stress in HCC. Redox Biol *24*, 101217. 10.1016/j.redox.2019.101217.

Ko, E., Seo, H.W., Jung, E.S., Ju, S., Kim, B.H., Cho, H., Kim, Y.J., Park, Y.M., Kim, J.S., and Jung, G. (2018). PI3Kdelta Is a Therapeutic Target in Hepatocellular Carcinoma. Hepatology *68*, 2285-2300. 10.1002/hep.30307.

Koivuluoma, S., Tervasmaki, A., Kauppila, S., Winqvist, R., Kumpula, T., Kuismin, O., Moilanen, J., and Pylkas, K. (2021). Exome sequencing identifies a recurrent variant in SERPINA3 associating with hereditary susceptibility to breast cancer. Eur J Cancer *143*, 46-51. 10.1016/j.ejca.2020.10.033.

Lenz, K.M., and Nelson, L.H. (2018). Microglia and Beyond: Innate Immune Cells As Regulators of Brain Development and Behavioral Function. Front Immunol *9*, 698. 10.3389/fimmu.2018.00698.

Liguori, I., Russo, G., Curcio, F., Bulli, G., Aran, L., Della-Morte, D., Gargiulo, G., Testa, G., Cacciatore, F., Bonaduce, D., and Abete, P. (2018). Oxidative stress, aging, and diseases. Clin Interv Aging *13*, 757-772. 10.2147/CIA.S158513.

Ljubisavljevic, S. (2016). Oxidative Stress and Neurobiology of Demyelination. Mol Neurobiol *53*, 744-758. 10.1007/s12035-014-9041-x.

Ma, Q. (2013). Role of nrf2 in oxidative stress and toxicity. Annu Rev Pharmacol Toxicol *53*, 401-426. 10.1146/annurev-pharmtox-011112-140320.

Ortega, L., Balboa, F., and Gonzalez, L. (2010). alpha(1)-Antichymotrypsin deficiency associated with liver cirrhosis. Pediatr Int *52*, 147-149. 10.1111/j.1442-200X.2009.02950.x.

Rupprecht, C., Rupprecht, R., and Rammes, G. (2021). C1q, a small molecule with high impact on brain development: putative role for aging processes and the occurrence of Alzheimer's disease. Eur Arch Psychiatry Clin Neurosci *271*, 809-812. 10.1007/s00406-021-01273-9.

Sanchez-Navarro, A., Gonzalez-Soria, I., Caldino-Bohn, R., and Bobadilla, N.A. (2021). An integrative view of serpins in health and disease: the contribution of SerpinA3. Am J Physiol Cell Physiol *320*, C106-C118. 10.1152/ajpcell.00366.2020.

Santamaria, M., Pardo-Saganta, A., Alvarez-Asiain, L., Di Scala, M., Qian, C., Prieto, J., and Avila, M.A. (2013). Nuclear alpha1-antichymotrypsin promotes chromatin condensation and inhibits proliferation of human hepatocellular carcinoma cells. Gastroenterology *144*, 818-828 e814. 10.1053/j.gastro.2012.12.029.

Schuller, U., Heine, V.M., Mao, J., Kho, A.T., Dillon, A.K., Han, Y.G., Huillard, E., Sun, T., Ligon, A.H., Qian, Y., et al. (2008). Acquisition of granule neuron precursor identity is a critical determinant of progenitor cell competence to form Shh-induced medulloblastoma. Cancer Cell *14*, 123-134. 10.1016/j.ccr.2008.07.005.

Sergi, D., Campbell, F.M., Grant, C., Morris, A.C., Bachmair, E.M., Koch, C., McLean, F.H., Muller, A., Hoggard, N., de Roos, B., et al. (2018). SerpinA3N is a novel hypothalamic gene upregulated by a high-fat diet and leptin in mice. Genes Nutr *13*, 28. 10.1186/s12263-018-0619-1.

Vicuna, L., Strochlic, D.E., Latremoliere, A., Bali, K.K., Simonetti, M., Husainie, D., Prokosch, S., Riva, P., Griffin, R.S., Njoo, C., et al. (2015). The serine protease inhibitor SerpinA3N attenuates neuropathic pain by inhibiting T cell-derived leukocyte elastase. Nat Med *21*, 518-523. 10.1038/nm.3852.

Wagner, K.D., and Wagner, N. (2022). The Senescence Markers p16INK4A, p14ARF/p19ARF, and p21 in Organ Development and Homeostasis. Cells *11*. 10.3390/cells11121966.

Wang, Y., Zhang, S., Lan, Z., Doan, V., Kim, B., Liu, S., Zhu, M., Hull, V.L., Rihani, S., Zhang, C.L., et al. (2022). SOX2 is essential for astrocyte maturation and its deletion leads to hyperactive behavior in mice. Cell Rep *41*, 111842. 10.1016/j.celrep.2022.111842.

Zamanian, J.L., Xu, L., Foo, L.C., Nouri, N., Zhou, L., Giffard, R.G., and Barres, B.A. (2012). Genomic analysis of reactive astrogliosis. J Neurosci *32*, 6391-6410. 10.1523/JNEUROSCI.6221-11.2012.

Zengeler, K.E., and Lukens, J.R. (2021). Innate immunity at the crossroads of healthy brain maturation and neurodevelopmental disorders. Nat Rev Immunol *21*, 454-468. 10.1038/s41577-020-00487-7.

Zhang, S., Wang, Y., Zhu, X.Q., Song, L.Y., Zhan, X.H., Ma, E., McDonough, J., Fu, H., Cambi, F., Grinspan, J., and Guo, F.Z. (2021). The Wnt Effector TCF7l2 Promotes Oligodendroglial Differentiation by Repressing Autocrine BMP4-Mediated Signaling. Journal of Neuroscience *41*, 1650-1664. 10.1523/Jneurosci.2386-20.2021.

Zhao, J., Feng, C., Wang, W., Su, L., and Jiao, J. (2022). Human SERPINA3 induces neocortical folding and improves cognitive ability in mice. Cell Discov *8*, 124. 10.1038/s41421-022-00469-0.